IEEE Open Journal of
Industry Applications

Received 4 January 2024; revised 16 April 2024; accepted 7 May 2024. Date of publication 13 May 2024;
date of current version 21 May 2024. The review of this article was arranged by Associate Editor Giulia Tresca.

Digital Object Identifier 10.1109/OJIA.2024.3400208

DC Arc Flash Measurements From a 1000 V Valve Regulated Lead Acid Battery System

NICOLAUS JENNINGS [1] (Graduate Student Member, IEEE), DAVID WETZ [1] (Senior Member, IEEE), RICK LANGLEY [2], NANCY LAFLAIR [2], AND JOHN HEINZEL [3]

[1]Pulsed Power and Energy Laboratory, University of Texas at Arlington, Arlington, TX 76019-9800 USA
[2]Electric Power Research Institute, Knoxville, TN 28262-8550 USA
[3]Naval Surface Warfare Center, Philadelphia, PA 19112 USA

CORRESPONDING AUTHOR: DAVID WETZ (e-mail: wetz@uta.edu)

This work was supported in part by the ONR under Grant N00014-21-1-2783, in part by NAVSEA CPSD through Naval Engineering Education Consortium under Grant N00174-22-1-0023, and in part by the ONR and executed on Army C5ISR Contract DOTC-17-01-INIT1218.

ABSTRACT As the Navy moves forward with implementing electrochemical energy sources in their power systems, a need to understand the hazards present to electric workers comes to light. Understanding the effects these sources have on arc flash hazards drives the need to study relevant energy sources that are deployed on naval platforms. A 1000-V valve regulated lead acid (VRLA) battery system presents the greatest need to study as incident energy models can suggest dramatic personal protective equipment (PPE) especially with the inclusion of scale factors. As a part of a collaborative effort between the Electric Power Research Institute (EPRI) and the University of Texas at Arlington (UTA) arc flash studies of VRLA battery systems at voltages as high as 936 V have been performed. Findings show that below 800 V, the battery sourced incident energy as high as 0.26 cal/cm^2. Above 800 V, incident energy surpassed 1.2 cal/cm^2 and approached category 1 PPE (4 cal/cm^2). A model derived from this work is used to emphasize the impact enclosure based scale factors have on incident energy estimates. This work has also compared relevant dc incident energy models to the measured incident energy sourced from this battery system.

INDEX TERMS Arc flash, electrochemical energy storage, incident energy, lead acid batteries, personal protective equipment (PPE).

I. INTRODUCTION

The increasing need and use of electrochemical energy storage has raised environmental and safety concerns, especially regarding fire, explosion, and arc flash for a wide range of sectors. These sectors include residential, commercial/industrial, utility, and military applications. These future energy storage systems pursue differing technologies and battery chemistries and with this comes varying levels of applications. Consumer use of energy storage is more commonly found in electric vehicles and backup batteries for photovoltaic arrays with increasing demand for lithium-ion (Li-ion) technology. The choice for Li-ion batteries is driven by a comparatively high gravimetric energy density to other technologies. But with this metric comes hazardous Li-ion battery fires that detract from the widespread use of this technology. Energy storage in industrial and military applications is used in a broader array of applications, including uninterruptible power supplies (UPSs), power demand management, load buffering, and hybrid power systems that include a variety of traditional ac and dc power sources and loads. The type of electrochemistry technology will depend on the application and the scale of the system. In traditional medium and large UPS applications, the battery systems typically operate at 380 Vdc [1]. Study and application of energy storage in technologies in the military additionally consider the safety challenges that need to be addressed for those who will perform maintenance on these systems. Today, motivated by higher efficiency operations, there are applications being designed and installed with battery system terminal voltages up to 1000 Vdc [2]. The space constraints and limitations for some military applications, such as US Navy ships, have resulted in heightened interests and concerns for the safety of workers operating and

maintaining the high-voltage and high-capacity battery energy storage systems.

Electric workers operating around these electrochemical energy storage systems are exposed to hazards like electric shock, battery fires as mentioned before, and arc flash. The latter is associated with most fatalities among electric workers and occurs when two potentials of an electric system conduct and ionize the air in between the two points [3]. The ionization of air leads to a pressure wave due to the air rapidly expanding. In addition, energy is radiated away in the form of heat and light. The light produced by the arc is like that of arc welding and can cause temporary or permanent blindness if exposed to even for short periods of time. The extreme heat is released throughout the duration of the arc and can leave workers sustaining second-degree burns, permanent disfigurement, or fatally succumbing to the heat. This arc will persist as long as there is sufficient energy to continue conducting all while the arc rapidly changes. The source driving this arc influences the severity of the event and is exacerbated in electrochemical energy storage systems where there are difficulties in controlling the source. AC systems have inherent zero-crossing points that prove beneficial in halting the current. Whereas in dc systems, extinguishing an arc becomes difficult because they employ capacitors, photovoltaic arrays, or batteries that cannot be turned OFF. Effective means of detecting this hazard in dc systems have been demonstrated with sound and light measurements [4]. Arcs produce a distinct measurable sound that can be detected with microphones placed throughout the system. In addition, light can also be used to detect arcs at any point in the system. These measurements can be used to control electric breakers and, in combination with fuses, can reduce arc flash hazards.

Workers who perform maintenance downstream from a fuse are assured that hazard reduction measures are in place but workers who perform maintenance "inside" or upstream from the fuse or nearest protection device can only rely on some element inside the dc system fusing open and their arc flash rated personal protective equipment (PPE). Workers must perform maintenance inside the fuse in places where the potentials of the energy storage system are brought together in an electrical panel or box. With direct connections to the battery terminals, an arc flash event can form when a worker drops their tool, like a wrench, across buswork. Often, the wrench is pushed off from the electrical contacts eliminating the short condition. In this scenario, an arc is formed and the blast pressure is enough to prevent the wrench from welding to the buswork. However, in the instance that a tool were to weld itself to the buswork the wrench will act as the fault point in the system kindling an arc flash event. As the wrench heats up and melts an arc can form between the small air gap that has opened in the wrench [5]. This arc can self-extinguish due to convective or magnetic forces blowing the arc away, some element of the energy system can fuse open, or the energy storage system can no longer source the energy required to sustain the arc. Ultimately, a worker can only rely on their PPE protecting them from the potential harm of these events. This PPE is selected based on estimations or calculation of the heat released from the arc, measured as incident energy, that can significantly reduce the damage suffered by the worker.

The body of work surrounding the study of arc flash has been focused on 3-phase ac systems with standards like IEEE 1584 and NFPA 70E established to address arc flash hazards for workers [6], [7]. NFPA 70E goes further to provide recommendations for dc systems but uses methods that can vastly overestimate the PPE required. Two methods are employed in 70E for dc systems: PPE category method and incident energy analysis method. First, the PPE category method is designed to provide electrical workers with an idea of PPE is required within the working area and what boundary area is determined for that electrical system. This boundary area is a region where the minimum sustained incident energy is 1.2 cal/cm^2. This incident energy value is the minimum amount to sustain second-degree burns for personnel not wearing the proper PPE [7], [8]. Second, the incident energy analysis method directly estimates the incident energy through a method using a maximum power calculation. For work that takes place inside battery cabinets, the incident energy analysis method is the only one that can be applied. Since this method assumes that the maximum power is delivered to the arc from the source, the incident energy values that are generated tend to be overestimates of incident energy values that are actually measured [10]. This leads to electrical workers over-encumbered with PPE.

The thrust of work for dc systems is focused on ac rectified sources and computational magnetohydrodynamics, which are used to develop dc incident energy models [11], [12]. These incident energy models are a starting point for developing standards to address these systems but do not model the effects of electrochemical energy sources. This drives a need to study relevant power systems to understand the potential hazards from battery systems currently employed in shipboard power systems. The Electric Power Research Institute (EPRI) in Knoxville, Tennessee and the University of Texas at Arlington (UTA) Pulsed Power and Energy Laboratory have collaborated to study dc arc flash sourced from valve regulated lead acid (VRLA) battery systems up to 960 Vdc. Experiments performed at EPRI were conducted in voltage ranges of 156–960 V primarily studying incident energy. At UTA, experiments were conducted at 130 and 260 V studying light intensity and sound pressure in addition to incident energy. This article will present the work to date covering the measurement of dc arc flash phenomena from VRLAs and compare the findings with incident energy models proposed in the literature.

This article begins with the development of a battery model in Section II to discuss the electrochemistry and methodologies used to determine internal resistance. Section III covers the measurement devices and enclosure configurations used at both facilities. Section IV covers the data collection of arc flash phenomena and includes a comparison of arc power models to a calculated average power. Finally, Section V

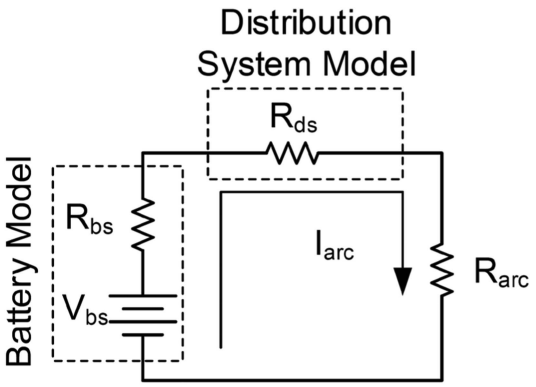

FIGURE 1. Simple battery model and arc flash test circuit.

compares measured incident energy with commonly used dc incident energy estimation methods.

II. BATTERY MODEL

After analysis of more than 1800 arc fault experiments used to develop the 2018 revision of IEEE 1584 [6], it was observed that arc current is dependent upon the available fault current. Available fault current is limited in electrochemical energy sources, like the VRLAs in this study, because of the internal resistance of the source. Thus, the effort was directed toward studying larger module count systems over single modules. A simple battery model, shown in Fig. 1, is typically used in both the maximum power [13] and ammerman model [14] for incident energy analyses and was informed in this work from the experimental data. The previous two incident energy analysis methods are highlighted in the discussion of arc power methods in Section IV-C.

Of the many test procedures used to characterize the internal resistance of the battery, two were chosen. First, UTA performed controlled near short circuit discharges to evaluate internal resistance. These experiments were performed utilizing a low-impedance test stand that connects 60 high-power MOSFETs in parallel with the battery. When all of the FETs are ON, the stand can have an impedance as low as 400 $\mu\Omega$. Fig. 2 shows the VRLA battery undergoing a near short fault on the test stand. The FETs were closed for two seconds to study the fall-off in voltage in the time that personnel could move away from the arc. Finding the internal resistance of the battery uses the initial voltage of the battery V_i, conduction voltage of the battery V_c, and conduction current I_c. The internal resistance of the battery is found by taking the difference in initial and conduction voltage divided by the conduction current. From these initial experiments, the VRLA internal resistance was found to be around 2.65 mΩ.

For stationary lead acid batteries, the standard test method for determining a battery's short circuit current and dc internal resistance can be found in the IEC 60896-21 [15]. This method calls for testing the battery under two specific loading conditions. The two loading conditions are based on the 10-h discharge rate of the battery, known as I_{10}. The first load test

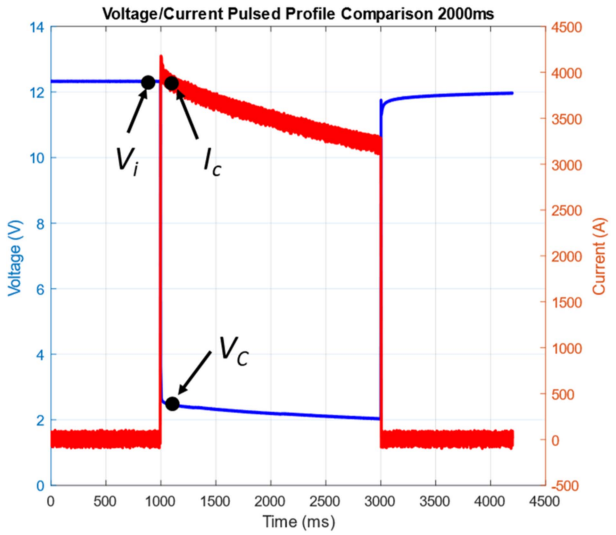

FIGURE 2. Two-second near short pulse of VRLA with voltage across the battery terminals in blue and current in red.

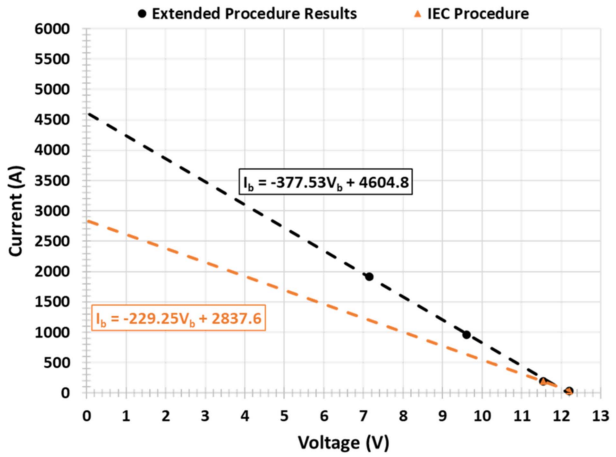

FIGURE 3. Line of best fit through various discharge currents with specific conduction voltage.

condition is defined as a current equal to $4 \times I_{10}$. The second test load condition is defined as a current equal to $20 \times I_{10}$. In [16], researchers at C&D Technologies describe a method that more accurately represents the actual short-circuit current of lead-acid batteries. They argue that the test loads are too low and will result in underpredictions of the short-circuit current in lead acid batteries. They showed that a more accurate methodology would include higher test load conditions, such as $100 \times I_{10}$ and $200 \times I_{10}$.

After studying near short circuit conditions, UTA and EPRI decided to use a second method implementing the higher test load recommendations on the VRLA battery. The battery is rated at 96 Ah at 13 Vdc. Results of the battery test are shown in Fig. 3. The orange line shows the straight-line approximation when only the two lower current test points are used to characterize the short-circuit current of the battery. The black line shows the impact of using the two higher test loads. The

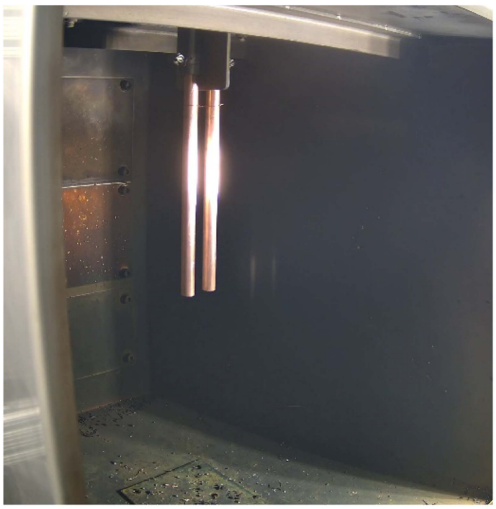

FIGURE 4. EPRI enclosure with vertical copper electrodes.

FIGURE 5. UTA enclosure with vertical copper electrodes.

difference is nearly 1800 A higher. The internal resistance of the battery is the negative inverse of the slope of the black dashed line in Fig. 3 or 2.65 mΩ.

III. MEASUREMENT SUITE

In the worst-case scenario, a maintenance worker is exposed to the full potential of the battery energy storage working upstream from fault-clearing devices. This instance occurs inside a combiner box where multiple potentials are brought together from the battery. Electrical enclosures range widely in size, gap distances between energized components vary greatly, and orientations of energized components are numerous.

A. ENCLOSURES AND ELECTRODES

EPRI and UTA constructed similar but distinct electrode and enclosure configurations. EPRI opted for a 508 mm^3 (20 in^3) stainless steel enclosure with vertical electrodes. The 12.7 mm (0.5 in) diameter copper rod electrodes were positioned vertically inside the enclosure so that the tips of the electrodes were positioned in the center. This enclosure volume aligns with the enclosure size for low-voltage switchgear listed in Table 8 of IEEE 1584 [6]. A photograph of this enclosure is shown in Fig. 4. With a slightly less volume, UTA opted for a 457 mm × 457 mm × 609.6 mm metal enclosure with opposing copper block electrodes as shown in Fig. 5. At a slightly less volume, UTA opted for a 457 mm × 457 mm × 609.6 mm metal box used with vertical electrodes mounted at the back of the box capable of gap distance adjustment. At both facilities, the interior is painted flat black and the electrodes are replaced for each experiment.

B. CALORIMETER BOARD

Identifying proper PPE requires understanding the incident energy workers may face. IEEE 1584 and other standards use copper calorimeters to measure incident energy. Using the calorimeter design outlined in ASTM F-1959 [17], a board made of G10 fiberglass mounts thirteen calorimeters 45.7 cm

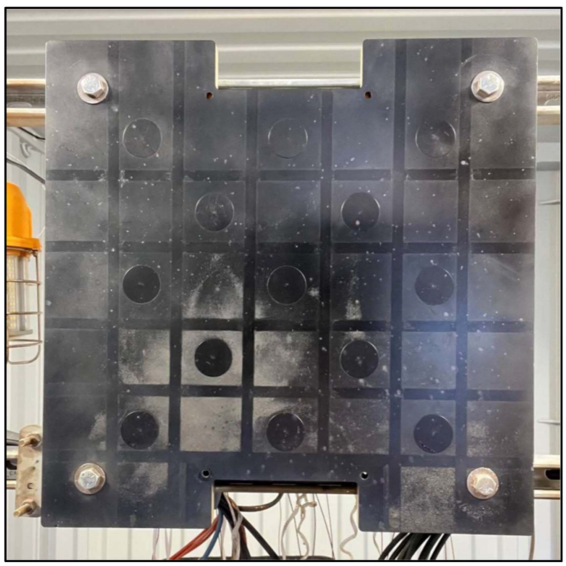

FIGURE 6. Calorimeter board with 13 calorimeters after numerous arc flash experiments.

(18 in) away from the arc location shown in Fig. 6. Temperature data collection of the thermocouples attached to the back of the calorimeters exceed the standard's requirements and care is taken to clean the sensors between experiments. Two additional thermocouples were utilized during each test for ambient temperature readings.

C. DATA ACQUISITION AND TEST MEASUREMENTS

During each arc flash experiment, the temperature readings for each calorimeter and thermocouple were recorded at a rate of 500 samples per second. In addition to the calorimeter measurements, infrared cameras were positioned to measure and record the surface of the calorimeterboard. The infrared

FIGURE 7. VRLA battery bank used in experiments performed at EPRI.

videos served as validation and backup for the calorimeter measurements. Fig. 6 shows a photograph of a calorimeter board used in the experiments.

Arc voltage was measured between the positive and negative electrode terminals on the outside of the enclosure. Battery (or arc) current measurements were recorded for each battery string. The arc voltage and arc current were recorded at 2M samples per second during each experiment.

IV. EXPERIMENTAL RESULTS

Experiments at both facilities focused on 12.7 mm electrode gap distances and smaller and larger gap distances were briefly studied. At UTA, 6.35 mm and 3.2 mm gap distances were studied with an emphasis on understanding the impact gap distance has on incident energy at lower voltages. At EPRI, additional effort was focused on greater gap distances (19 mm and 25 mm) to study with higher voltages. The batteries, in Fig. 7, were kept indoors and were maintained at room temperature between 18 and 25 °C (64.4 °F–77 °F). Different strings of batteries were used between experiments but performance across all strings was similar. Table 1 outlines the tests performed across both facilities with over 106 VRLA experiments performed to date.

Voltage and current measurements are captured with sufficient temporal resolution so as to observe arc dynamics. An example of this electrical data is shown in Fig. 8. This snippet of data is from a 130 V (10S/1P) arc flash incident that lasted 11.5 ms at a gap distance of 6.35 mm.

A. INCIDENT ENERGY

Incident energy measurements in Fig. 9 are shown up to the maximum battery configuration at a gap distance of 12.7 mm. Single string and two string configurations show no difference at potentials below 500 V. Above 500 V, incident energy develops more and surpasses 1.2 cal/cm^2 at 858 V with an experiment reaching 1.59 cal/cm^2. At 936 V, an experiment recorded 3.67 cal/cm^2 approaching a 4 cal/cm^2 PPE category. This test was cut short due to a battery blowing open and

TABLE 1. Arc Flash Testing Summary

Voltage	Battery Configurations	Number of Experiments	Gap Distances Studied (mm)
130 V	10S/1P 10S/2P	12 – 1P & 12 – 2P	3.2, 6.35, 12.7
156 V	12S/1P 12S/2P	6 – 1P & 5 – 2P	12.7
234 V	18S/1P 18S/2P	4 – 1P & 4 – 2P	12.7
260 V	20S/1P 20S/2P	12 – 1P	3.2, 6.35, 12.7
312 V	24S/1P 24S/2P	4 – 1P & 4 – 2P	12.7
390 V	30S/1P 30S/2P	4 – 1P & 2 – 2P	12.7
468 V	36S/1P 36S/2P	11 – 1P & 6 – 2P	6.35, 12.7, 19, 25
546 V	42S/1P	4 – 1P	12.7
624 V	48S/1P	4 – 1P	12.7
702 V	54S/1P	4 – 1P	12.7
780 V	60S/1P	4 – 1P	12.7
858 V	66S/1P	2 – 1P	12.7
936 V	72S/1P	2 – 1P	12.7

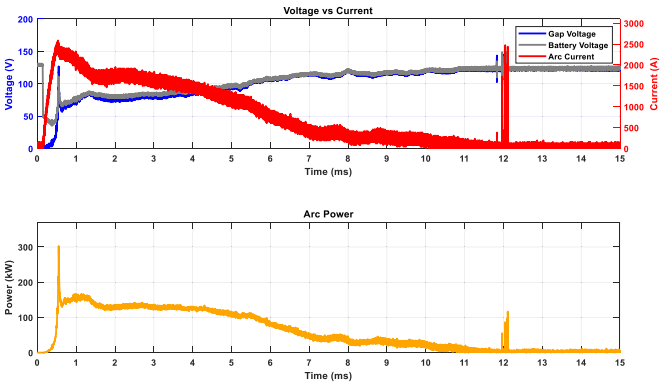

FIGURE 8. Voltage and current measurements from a 130-V arc flash experiment shown with instantaneous power.

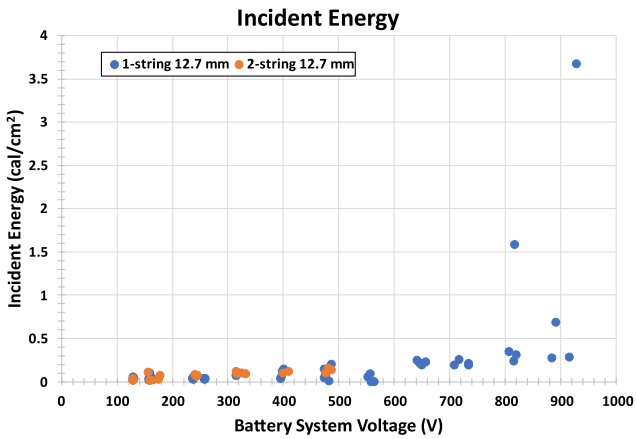

FIGURE 9. Measured incident energy from one and two-string VRLA battery arc flash experiments recorded at 12.7 mm gap distance.

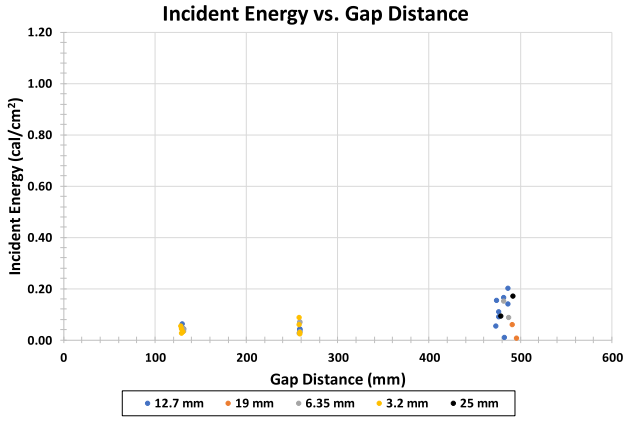

FIGURE 10. Comparison of incident energy measurements across various gap distances showing 12.7, 19, 6.35, 3.2, and 25 mm gap distances.

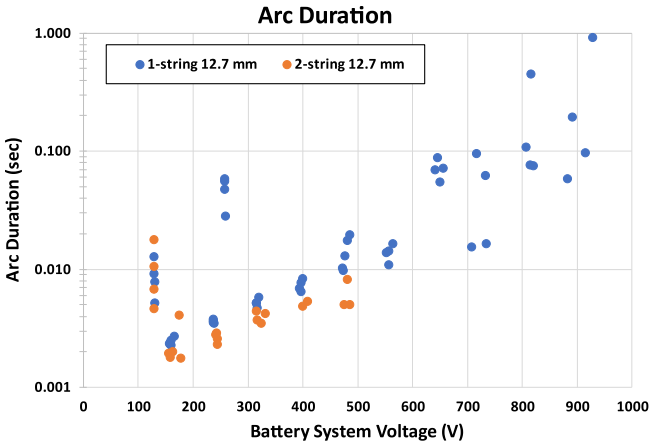

FIGURE 11. Arc duration versus battery system voltage across different string counts.

breaking the circuit. Had this event continued, surely more incident energy would have been recorded and while these experiments replicate environments with no fuse protections, sources themselves can act as the opening mechanism for an arc flash event. The remaining experiments at these potentials exhibit lower incident energy measurements than the outlier events discussed. In Fig. 10, smaller gap distances did not contribute significantly to incident energy at voltages below 260 V. At around 468 V, variance in gap distance did not lead to a noticeable increase in incident energy. The battery has a significant drop in voltage in these arc fault scenarios which reduces the potential across the gap.

B. ARC DURATION

A strong determinant of incident energy is the duration of the arc fault. Figs. 11 and 12 outline the arc durations measured from each experiment compared to the respective battery voltage and incident energy. At potentials studied at UTA, arc durations are significantly greater than similar voltages studied at EPRI. Studying the average arc current, UTA's batteries put out less current than EPRI's which most likely comes down to battery condition. Experiments below 500 V

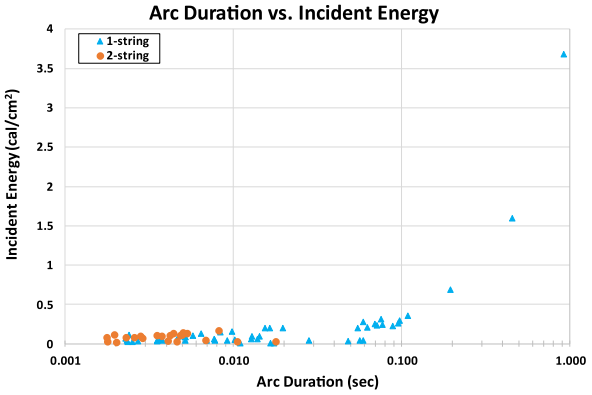

FIGURE 12. Incident energy versus arc duration for two and one string arrangements with arc duration plotted on a logarithmic scale.

tend to stay below 20 ms excluding UTA's data. Above 500 V, arc durations increase significantly with battery system voltage. In Fig. 11, two string experiments demonstrated slightly lower arc durations than single-string experiments at the same voltage. This is strongly driven by a near doubling in arc current through the circuit leading to the arc blowing out due to magnetic forces. In Fig. 12, all durations less than 150 ms recorded less than 0.5 cal/cm^2.

C. ARC POWER

Using the electrical data captured, average arc power is found by taking the average of the instantaneous arc power over the arc duration starting just right after reaching steady state. Since arc power is a relatively stable metric throughout the duration, it provides a fair value of comparison. Two models of interest are those proposed by Doan [13] and Ammerman et al. [14]. The maximum power method proposed by Doan and incorporated in NFPA 70E, estimates the incident energy of a dc arc flash. This method assumes that the source resistance and distribution system resistance are equal to the arc resistance. The model proposed by Ammerman, through empirical analysis, utilizes system characteristics and iteratively solves for arc power. The maximum power method uses the following equation incorporating circuit parameters shown in Fig. 1.

$$P_{\max} = \frac{V_{\text{bs}}^2}{4\,(R_{\text{ds}} + R_{\text{bs}})}. \tag{1}$$

In (1), V_{bs} is the battery system voltage, R_{ds} is the equivalent resistance of the distribution system (3 mΩ for EPRI and 0.1 mΩ at UTA), and R_{bs} is the internal resistance of the battery. The Ammerman model uses (2) and (3) solving for arc power. In this case, bolted fault current and battery system voltage were used to iteratively solve for arc power

$$V_{\text{arc}} = (20 + 0.534 * 12.7)\, I_{\text{arc}}^{0.12} \tag{2}$$

$$R_{\text{arc}} = \frac{(20 + 0.534 * 12.7)}{I_{\text{arc}}^{0.88}}. \tag{3}$$

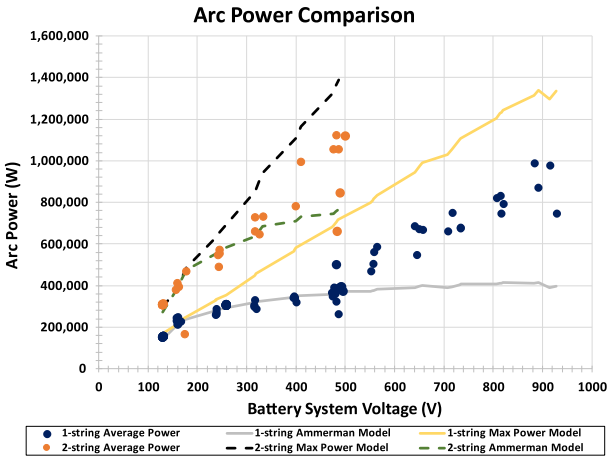

FIGURE 13. Comparison of measured arc power to commonly used dc arc flash models.

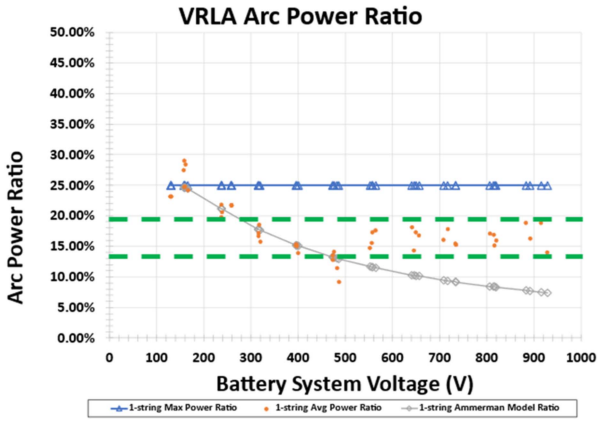

FIGURE 14. Arc power ratio for one string VRLA experiments. Green dashed lines bound a region where the arc power ratio lies beyond 500 V.

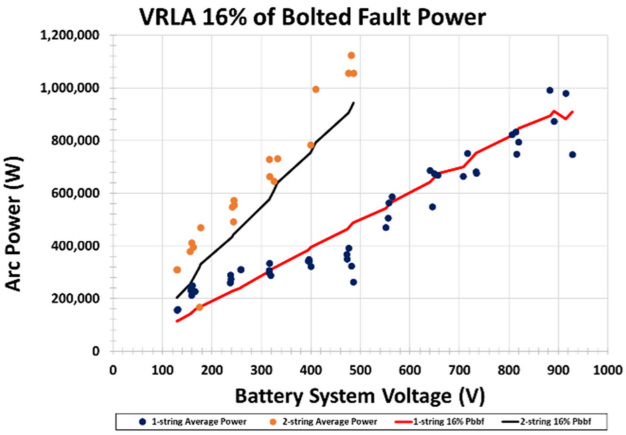

FIGURE 15. Arc power model fit to 16% of bolted fault power from VRLAs.

Application of these arc power models is shown in Fig. 13. In a single string configuration, average arc power aligned with Ammerman model below 500 V. Above this potential, arc power was in between the maximum power model and Ammerman model. This behavior is likely due to the very short duration arcs that occur below 500 V supported by the arc duration noticeably increasing after 500 V. For a two-string configuration, arc power follows the Ammerman model closely for battery voltages below 330 V, above this voltage, average arc power again is between the Ammerman model and maximum power model.

Upon closer inspection of Fig. 13, a linear trend in arc power is apparent at voltages above 500 V. Finding this trend begins by using a metric called bolted fault power P_{bbf} defined as the following:

$$P_{\text{bbf}} = V_{\text{bs}} I_{\text{bbf}} = \frac{V_{\text{bs}}^2}{(R_{\text{ds}} + R_{\text{bs}})} \tag{4}$$

where V_{bs} is the battery system voltage, I_{bf} is the bolted fault current, R_{ds} and R_{bs} are the distribution system and battery system resistance, respectively. Using (4), an arc power ratio is calculated for the methods described previously and graphically presented in Fig. 14. Here, the maximum power model is 25% of (4) for all voltages and the adherence to the Ammerman model is seen for measurements at voltages below 500 V. Above 500 V, two green dashed lines define a region where the arc power ratio for average power is between. The distribution of these points is spread throughout the bounds but a line through 16% ensured that half of the ratios were above, and half were below. Then, multiplying (4) by 16%, a line of best fit through one and two-string average arc power is formed in Fig. 15. For the two-string experiments, this model underestimates the arc power requiring a higher percentage. The use of this arc power model will be discussed in Section V.

V. IE MODEL COMPARISON

Incident energy models assume the power of the arc radiates in an isotropic manner. A distance of 45.7 cm (18 in) away is termed the working distance and is where most of the exposed body would be when performing maintenance. Then using the arc power from the models presented, the following equation can be used to calculate the open-air arc incident energy:

$$\text{IE}\left(\frac{\text{cal}}{\text{cm}^2}\right) = \frac{P_{\text{arc}} * t_{\text{arc}}}{4\pi D^2} * 0.239 \frac{\text{cal}}{J} \tag{5}$$

where P_{arc} is the calculated arc power, t_{arc} is the measured arc duration, and D is the distance from the arc to the calorimeter board. Implementing the arc powers discussed previously, Fig. 16 shows the incident energy comparison for the single-string system and Fig. 17 shows the two-string comparison. The maximum power model underestimates incident energy at voltages below 500 V in both string configurations and overestimates beyond 500 V for a single-string configuration. This is likely explained by the increase in arc duration noted earlier beyond 500 V. The greatest incident energy the maximum power model estimated was 11.21 cal/cm^2 against a measured 3.67 cal/cm^2. Ammerman's model for durations

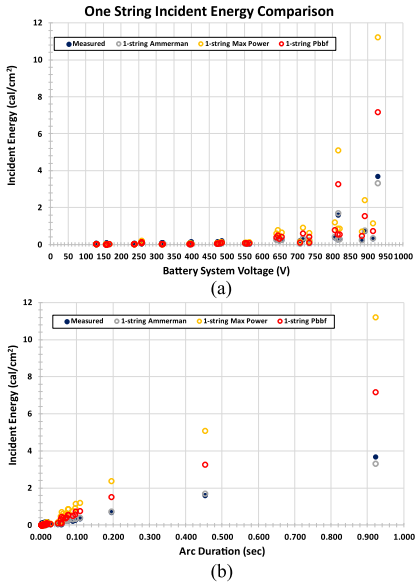

FIGURE 16. Incident energy calculations from models presented in the text compared to measured values at one string with a gap distance of 12.7 mm. The incident energy values are plotted against (a) battery system voltage and (b) arc duration.

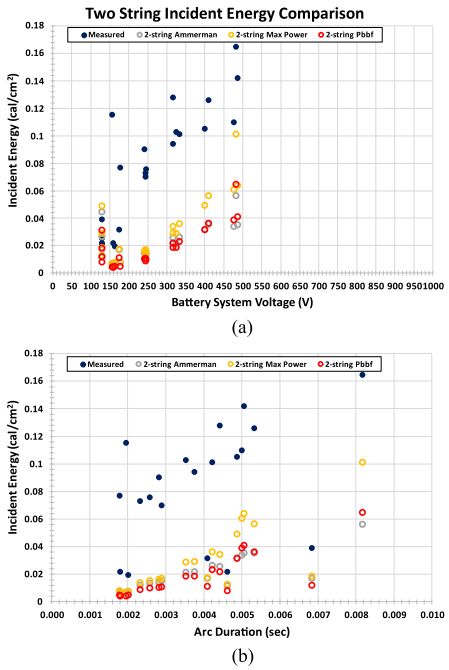

FIGURE 17. Incident energy calculations from models presented in the text compared to measured values at two strings with a gap distance of 12.7 mm. The incident energy values are plotted against (a) battery system voltage and (b) arc duration.

greater than 50 ms aligned with the incident energy measured. For the greatest incident measured, this model slightly underestimated it to be 3.33 cal/cm^2. The model completely underestimates incident energy for durations less than 50 ms; however, in this scenario, measured values pose little risk to workers.

The Ammerman model agrees with the measured data for longer durations, but the incident energy model used with it and all others propagate the energy in a perfect sphere not taking into account an enclosure. To fit the bolted fault power model to the measured data, a scale factor of 0.5 would be applied to achieve comparable results to the measured data. This means that, as opposed to an arc in the open air, the enclosure absorbs half of the energy leaving the box discounting any potential reflection from inside the box. Further, if multipliers were to be applied because an enclosure was used, predicted incident energy could certainly reach PPE categories that would be overly conservative. Thus, how an enclosure contributes to measured incident energy with any potential reflections or absorption in the material is needed. Studies of enclosure geometry's effect on the incident have been applied to 3-phase systems but lack standing in dc systems.

VI. CONCLUSION

DC arc flash experiments sourced from VRLA batteries up to 1000 V have been discussed in this article. While it can be said for this battery system that incident energy values posed some risk to workers below 800 V, broadly applying these results is not the aim of this work. All sorts of battery technologies have different capacities, internal resistance, short circuit currents, nominal voltage, and many other attributes that lead to different arc flash risks. Models discussed throughout the literature have been applied to this work and it was shown that the maximum power model available in NFPA 70E vastly overestimates the incident posed by this battery system. The Ammerman model applied aligned best with the work presented here and shows promise for work in future battery systems. However, the application of these models is based on the open-air arc assumption, which does not include potential reflections or absorption from the enclosure itself. Future work to address this concern and work towards studying other dc electrochemical energy sources is needed.

ACKNOWLEDGMENT

The opinions and findings here are those of the authors and may not reflect the views and opinions of ONR.

Conflict of Interest Statement: David Wetz is a paid consultant for Commonwealth Technology Incorporated, a subsidiary of HII Mission Technologies Corp. supporting the Pulsed Power and Plasma Physics Divisions of the Naval Research Laboratory. He is also a paid consultant with NoblisMSD supporting the Naval Surface Warfare Center—Philadelphia Division.

REFERENCES

[1] J. Inamori, H. Hoshi, T. Tanaka, T. Babasaki, and K. Hirose, "380-VDC power distribution system for 4-MW-scale cloud facility," in *Proc. IEEE 36th Int. Telecommun. Energy Conf.*, 2014, pp. 1–8, doi: 10.1109/INTLEC.2014.6972218.

[2] D. A. Wetz et al., "Design of 1000 V valve regulated lead acid (VRLA) and lithium-iron-phosphate lithium-ion (LFP-LI) battery test beds for driving high rate, pulsed loads," *Nav. Eng. J.*, vol. 129, no. 3, pp. 99–108, Sep. 2017.

[3] W.-J. Lee, T. Gammon, Z. Zhang, B. Johnson, and S. Vogel, "IEEE\/NFPA collaboration on arc flash phenomena research project," *IEEE Power Energy Mag.*, vol. 10, no. 2, pp. 116–123, Mar./Apr. 2012, doi: 10.1109/MPE.2014.2322302.

[4] W.-J. Lee, Z. Zhang, S.-H. Rau, T. Gammon, B. C. Johnson, and J. Beyreis, "Arc flash light intensity measurement system design," *IEEE Trans. Ind. Appl.*, vol. 51, no. 5, pp. 4267–4274, Sep./Oct. 2015, doi: 10.1109/TIA.2015.2431638.

[5] J. G. Hildreth and K. Feeney, "Arc flash hazards of 125 Vdc station battery systems," in *Proc. IEEE Power Energy Soc. Gen. Meeting*, 2018, pp. 1–5, doi: 10.1109/PESGM.2018.8586181.

[6] *IEEE 1584-2018 - IEEE Guide for Performing Arc-Flash Hazard Calculations*, IEEE Standard 1584-2018 (Revision of IEEE Standard 1584-2002), Nov. 11, 2018.

[7] *NFPA 70E Standard for Electrical Safety in the Workplace, 2021 Edition*, Standard NFPA 70E, National Fire Protection Association (NFPA), 2021.

[8] A. M. Stoll and M. A. Chianta, "Method and rating system for evaluations of thermal protection," *Aerosp. Med.*, vol. 40, pp. 1232–1238, 1969.

[9] M. Furtak and L. Silecky, *Evaluation of Onset to Second Degree Burn Energy in Arc Flash*. Richardson, TX, USA: IAEI, 2012.

[10] T. Gammon, W.-J. Lee, Z. Zhang, and B. C. Johnson, "A review of commonly used DC arc models," *IEEE Trans. Ind. Appl.*, vol. 51, no. 2, pp. 1398–1407, Mar./Apr. 2015, doi: 10.1109/TIA.2014.2347456.

[11] S.-H. Rau and W.-J. Lee, "DC arc model based on 3-D DC arc simulation," *IEEE Trans. Ind. Appl.*, vol. 52, no. 6, pp. 5255–5261, Nov./Dec. 2016, doi: 10.1109/TIA.2016.2587760.

[12] K. S. Y. Cheng, C. Samson, and S. Cress, "DC arc-flash testing and analysis at 600 V," in *Proc. IEEE Ind. Appl. Soc. Elect. Saf. Workshop*, 2020, pp. 1–6, doi: 10.1109/ESW42757.2020.9188330.

[13] D. R. Doan, "Arc flash calculations for exposures to DC systems," *IEEE Trans. Ind. Appl.*, vol. 46, no. 6, pp. 2299–2302, Nov./Dec. 2010, doi: 10.1109/TIA.2010.2070480.

[14] R. F. Ammerman, T. Gammon, P. K. Sen, and J. P. Nelson, "DC arc models and IE calculations," *IEEE Trans. Ind. Appl.*, vol. 46, no. 5, pp. 1810–1819, Sep./Oct. 201.

[15] IEC 60896-21, *Stationary lead-acid batteries – Part 21: Valve regulated types - Methods of test*, International Electrotechnical Commission, 2004.

[16] S. D. Gerner, P. D. Korinek, and T. E. Ruhlmann, "Calculated vs. actual short circuit currents for VRLA batteries. C&D battery technologies," 2023. [Online]. Available: https://www.sbsbattery.com/PDFs/VRLAshortCurrentsStorageBatterySystems.pdf

[17] *Standard Test Method for Determining the Arc Rating of Materials for Clothing*, Standard ASTM F1959/F1959-14E1, ASTM International, 2014.